

# THE CMS BEAM HALO MONITOR AT THE LHC: IMPLEMENTATION AND FIRST MEASUREMENTS

N. Tosi\*<sup>1</sup>, INFN Bologna, Italy

on behalf of the CMS Collaboration

<sup>1</sup>also at DIFA, Università di Bologna, Italy

## Abstract

A Cherenkov based detector system has been installed at the Large Hadron Collider (LHC), in order to measure the Machine Induced Background (MIB) for the Compact Muon Solenoid (CMS) experiment. The system is composed of forty identical detector units formed by a cylindrical Quartz radiator directly coupled to a Photomultiplier. These units are installed at a radius of 1.8 m and a distance of 20.6 m from the CMS interaction point. The fast and direction-sensitive signal allows to measure incoming MIB particles while suppressing the much more abundant collision products and albedo particles, which reach the detector at a different time and from a different direction. The system readout electronics is based on the QIE10 ASIC and a  $\mu$ TCA based back-end, and it allows a continuous online measurement of the background rate separately per each bunch. The detector has been installed in 2015 and is now fully commissioned. Measurements demonstrating the capability of detecting anomalous beam conditions will be presented.

## INTRODUCTION

The increase in beam energy and luminosity in the LHC Run II, started in 2015, also meant an increase in Machine Induced Background (MIB) for the experiments. The Beam Radiation Instrumentation and Luminosity (BRIL) project designed, built and currently operates detectors that measure Luminosity and MIB in several regions of the CMS experiment [1]. Among the MIB detectors are instruments designed for protection of the sensitive inner silicon detectors of CMS from severe beam loss events and others that detect when the MIB reaches levels that would interfere with data taking efficiency. The Beam Halo Monitor (BHM) [2] is the outermost such detector, and it is sensitive to beam gas interactions happening upstream of CMS as well as beam halo interactions with the upstream collimators.

## THE DETECTOR

### Concept

The BHM has to be able to detect and correctly identify MIB particles in the context of a particle flux dominated by products of high energy  $pp$  collisions. Detection and identification are based on techniques that exploit differences between MIB and other particles, combined into a single instrument:

- The MIB flux is dominated by muons, due to absorption and decay of other particle types, while a significant fraction of the  $pp$ -collision products is composed of neutral particles.
- The MIB originated from the incoming beam and the  $pp$ -collision products travel in opposite direction.
- At several locations along the beampipe, the MIB and the majority of  $pp$ -collision products arrive with maximal time separation between each other (exactly half of the bunch spacing, 12.5 ns).

A Cherenkov based detector can make use of all these characteristics, thanks to Cherenkov radiation being emitted promptly and in a known direction with respect to the particle trajectory.

### Detector Hardware

Each BHM detector unit is composed of a synthetic quartz cylinder, 100 mm long and 52 mm in diameter, acting as Cherenkov radiator, directly coupled to a fast, UV-sensitive photomultiplier tube (PMT). Particles travelling from the quartz towards the PMT (from right to left in Fig. 1) emit Cherenkov Light that reaches the photocathode. Particles travelling in the opposite direction also emit light, but this is instead absorbed by a layer of black paint applied to the free face of the quartz. These elements are enclosed in a three layer shielding to protect the PMT from the residual field of the CMS solenoid and to absorb the large flux of low energy particles present in the cavern.

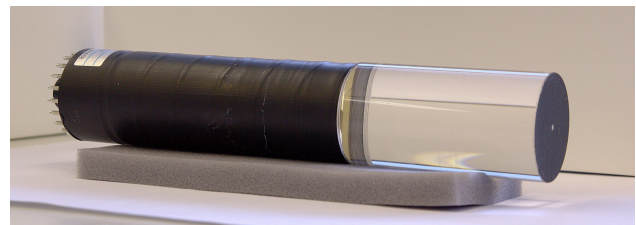


Figure 1: The active elements of the BHM detector unit: a 52 mm diameter quartz cylinder attached to an Hamamatsu R2059 photomultiplier.

The complete detector has twenty units on each end of CMS, mounted around the rotating shielding as shown in Fig. 2. They are located at a radius of 1.8 m and a distance of 20.6 m from the CMS interaction point and pointed towards the incoming beam. The large signal produced by the Hamamatsu R2059 PMT is brought to the readout electronics located in the service cavern via high bandwidth triaxial

\* nicolo.tosi@cern.ch

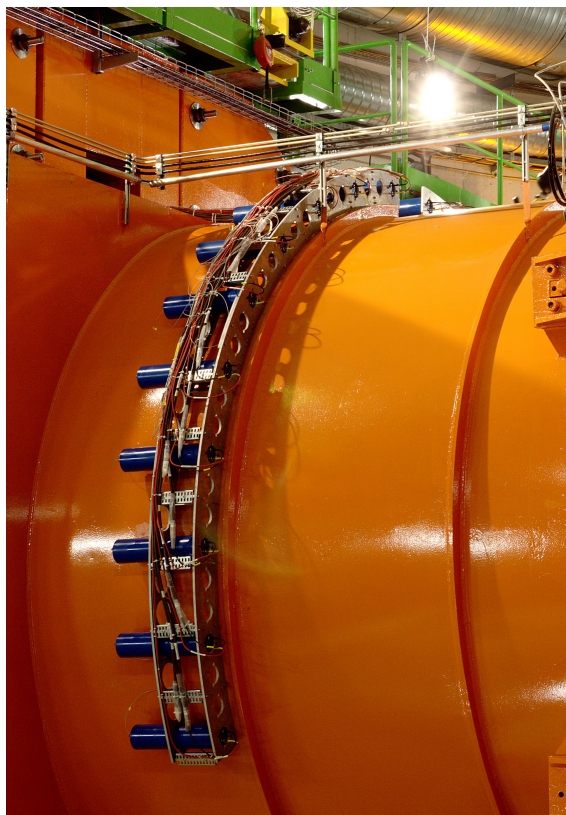


Figure 2: The BHM mounted on the rotating shielding around the beampipe in CMS.

cables, over a length of about 80 m. The PMT power supply and an LED pulse generator for monitoring are also located in the service cavern and connected to each unit with long cables and optical fibers, respectively.

### Readout

The readout electronics uses components developed for the Phase 1 upgrade of the CMS Hadron Forward Calorimeter (HF) [3]. This is composed of a front-end equipped with the QIE10 charge integrating ADC and TDC, as well as a  $\mu$ TCA based back-end.

The readout electronics collects hit count information separately per each bunch crossing (BX), with a further subdivision into four equal time slices in each BX. These counts are integrated over a period of  $2^{14}$  LHC orbits, equivalent to about 1.4 s, and are readout with no deadtime over a network connection. Amplitude spectra and single event waveforms can also be acquired for offline analysis and monitoring purposes.

## PERFORMANCE IN 2015 AND 2016

The BHM detector was installed in the CMS cavern in early 2015, and its readout electronics and data acquisition software were completed in the fall of the same year. A temporary, VME-based system provided the initial data readout.

### Initial Tests

Early during the commissioning of BHM, the LHC operators performed several experiments with the settings of the CMS tertiary collimator (TCTs) aperture. One such experiment was recorded and the MIB rates are shown in Fig. 3. This first measurement demonstrated the basic functionality of BHM.

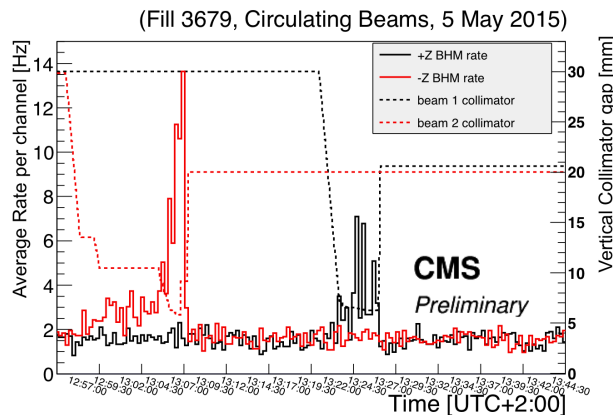


Figure 3: The BHM rates readout by VME scalers during collimators' setting: The dashed lines show the collimator gap for Beam 1 (black) and Beam 2 (red) TCT vertical collimators. The solid lines show the respective BHM average rate per channel for Beam 1 sensitive detectors (black) and Beam 2 sensitive detectors (red).

### Normal Operating Conditions

The discrimination of MIB is based on both a minimum amplitude threshold and a requirement on timing. One BX is subdivided into four time slices; the MIB is contained within one such slice, while collision products are distributed over all slices, due to large variations in their time of flight. An example of this distribution for a typical LHC fill is shown in Fig. 4.

Due to the distance of BHM from the interaction point, there is a significant difference in the proportion of collision products to MIB within a train of bunches. For a train of  $N$  colliding bunches, the BHM will measure 6 BX which contain only MIB hits,  $N - 6$  which contain hits from both MIB and  $pp$ -collisions and a further 6 with only collision hits, as shown on the right side of Fig. 5. Software corrections, calculated using these last 6 bunches in a train, are applied to the MIB time slice counts in the middle of the train to subtract the contamination from collision products. Two rates, averaged over all channels on each end and normalized for beam intensity, are calculated and published every *Lumi-Section* ( $\approx 23$  s).

**Angular Distribution** The shape of the LHC tunnel and beamline elements dictates the angular distribution of MIB around the beamline. A simulation of the flux, shown in Fig. 6, predicted a low flux of particles below the beamline (which was therefore not instrumented), due to absorption by

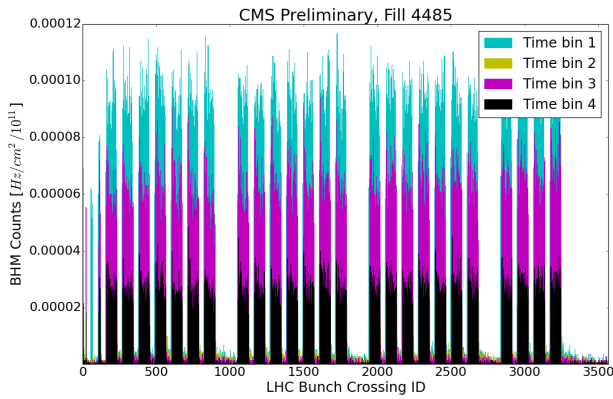


Figure 4: Bunch crossing occupancy histogram for one channel of BHM. MIB is expected to arrive at a time corresponding to bin 1 (cyan). This plot shows a fill with good beam conditions: all bunch trains produce a small and uniform MIB contribution.

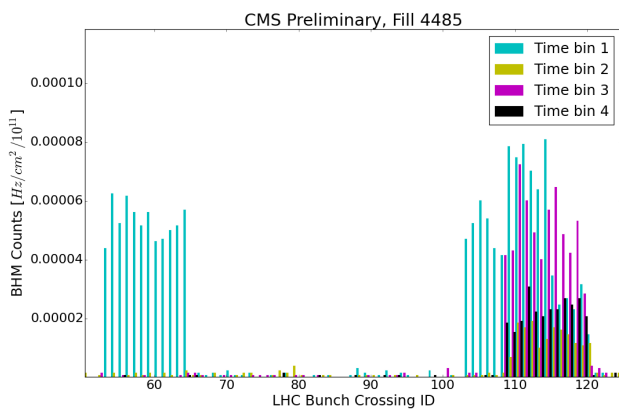


Figure 5: Detail of bunch crossing occupancy histogram for one channel of BHM. MIB is expected to arrive at a time corresponding to bin 1 (cyan). The peaks on the left side are purely MIB, produced by twelve non colliding bunches. The peaks on the right side include contributions from collision products of twelve bunches as well as MIB.

the tunnel floor, as well as an increased flux on the horizontal plane, in correspondence of the collimator jaws. Measurements, shown in Fig. 7 show a general agreement with the prediction.

### Collimator Scans

As part of the LHC Machine Development 310, several pilot bunches were excited provoking beam losses, while several collimators, including the TCTs adjacent to CMS, were adjusted across a wide range of apertures. As BHM is, by construction, especially sensitive to particles produced in interactions with the TCTs, a set of measurements (shown in Fig. 8) was taken in order to correlate the BHM measurement with the TCT aperture. An approximate exponential dependence on collimator aperture is observed, consistent with expectations.

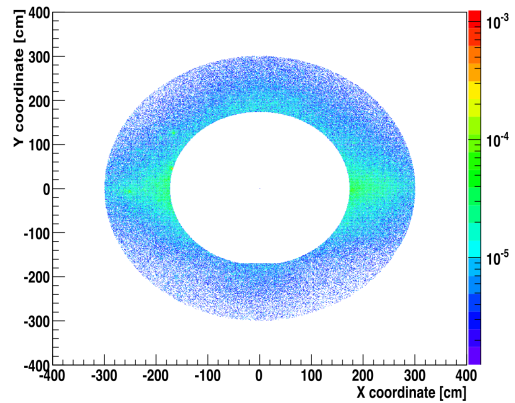


Figure 6: Simulation of the flux distribution in the XY plane of the MIB flux at the detector location ( $z = 20.6$  m), from [2].

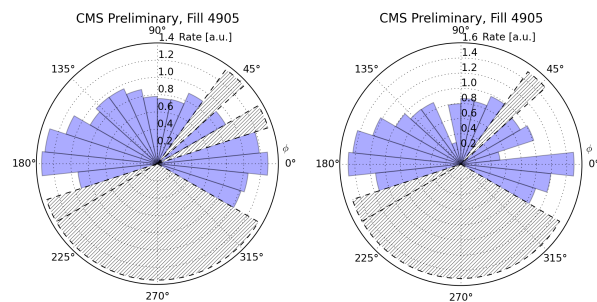


Figure 7: Angular distribution, around the beam pipe, of Machine Induced Background rate for Beam 1 (left) and Beam 2 (right). Each slice corresponds to one BHM channel. The rates are normalized to the average rate. The hatched areas are not instrumented or not available.

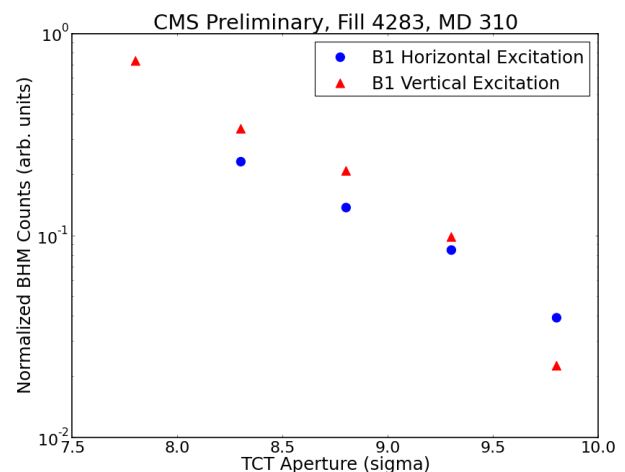


Figure 8: BHM count rates of all Beam 1 channels during Machine Development 310. An aperture scan of the tertiary collimators (TCTs) was performed while pilot bunches were excited. The ratio of the BHM count rate to the total beam loss, as measured by the Point 7 Beam Loss Monitor, is shown as a function of the TCT aperture.

### Beam Gas Test

A series of tests was conducted between May and June 2016 to determine the effect of beam gas interaction in the LHC experiments. In the first such test, during LHC fill 4905, a vacuum getter cartridge was heated, releasing trapped atoms into the beam, in the vicinity of the TCTs, at about 150 m from the CMS interaction point. Vacuum pressure, measured by several gauges, increased by five orders of magnitude with respect to normal operating conditions, and the MIB rate measured by BHM followed closely the evolution of the pressure over time, as can be seen in Fig. 9 and Fig. 10.

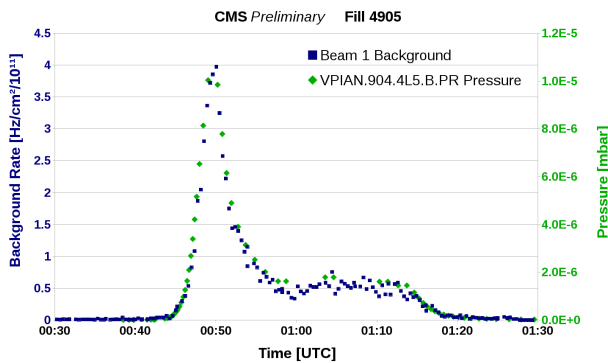


Figure 9: Time variation of MIB rates measured by BHM shown together with beampipe vacuum pressure, measured by the VPIAN.904.4L5 pressure sensor, for Beam 1.

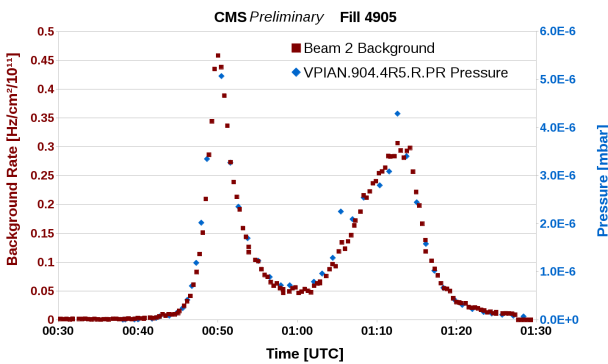


Figure 10: Time variation of MIB rates measured by BHM shown together with beampipe vacuum pressure, measured by the VPIAN.904.4R5 pressure sensor, for Beam 2.

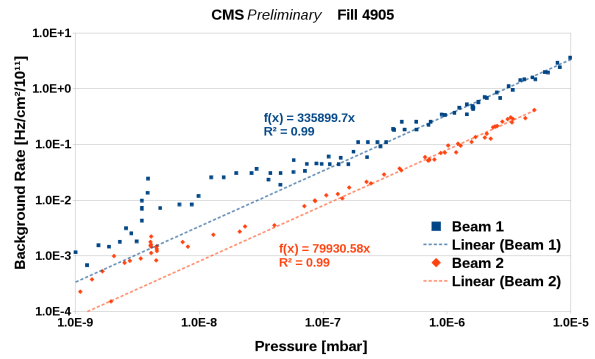


Figure 11: MIB rates versus beampipe Vacuum pressures, measured by the VPIAN.904 pressure sensor, for Beam 1 and Beam 2.

A linear correlation exists between measured pressure and MIB rate above a certain pressure, as shown in Fig. 11. Below  $\approx 10^{-7}$  mbar, additional contributions to MIB, such as the baseline halo background and occasional noise hits, spoil the linear dependence. Additional analyses are in progress to quantify the effect of the increasing MIB rate on the CMS data taking efficiency.

### CONCLUSIONS

The Beam Halo Monitor was installed in CMS at the beginning of 2015 to measure Machine Induced Background. It has met all its design requirements, and it is sensitive to increase of MIB beyond the normal operating conditions.

The detector is expected to remain operational and sensitive to beam background even with the upgrade to High Luminosity LHC.

### REFERENCES

- [1] A. Dabrowski *et al.*, “Upgrade of the CMS Instrumentation for luminosity and machine induced background measurements”, *Nucl.Part.Phys.Proc.*, vol. 273-275, p. 1147, 2016.
- [2] S. Orfanelli *et al.*, “A novel Beam Halo Monitor for the CMS experiment at the LHC” *J.Inst.* 10 no.11, P11011, 2015.
- [3] J. Mans *et al.*. “CMS Technical Design Report for the Phase 1 Upgrade of the Hadron Calorimeter” CERN, Geneva, Switzerland, CERN-LHCC-2012-015/CMS-TDR-010, 2012.